


# Congenital Indifference to Pain: An Illustrated Case Report and Literature Review

Ashkahn E Golshani<sup>1\*</sup>, Ankur A Kamdar<sup>2</sup>, Susanna C Spence<sup>1</sup>, Nicholas M Beckmann<sup>1</sup>

1. Department of Diagnostic and Interventional Imaging, University of Texas Health Science Center, Houston, USA

2. Department of Rheumatology, University of Texas Health Science Center, Houston, USA

\* **Correspondence:** Ashkahn Golshani, University of Texas Health Science Center at Houston, 6431 Fannin St. MSB 2.116, Houston, TX, 77030, USA

 Ashkahn.E.Golshani@uth.tmc.edu

Radiology Case. 2014 Aug; 8(8):16-23 :: DOI: 10.3941/jrcr.v8i8.2194

## ABSTRACT

Congenital indifference to pain is a rare and debilitating congenital disease. Individuals with the disorder may have one or a combination of sensory or autonomic deficits, which can range from lack of mechanical nociception, diminished ability to detect heat and cool stimulation, to the devastating and fatal form which includes autonomic dysfunction. It is important for radiologists to be able to recognize the radiographic presentations of this rare disorder, as delay in diagnosis can lead to extensive and sometimes unnecessary workup. We present a case of congenital indifference to pain initially interpreted as a mass of the distal femur.

## CASE REPORT

### CASE REPORT

An 8 year old girl presented with right knee pain, reporting that she recently fell from her bed. Upon further questioning she revealed that the pain had begun months prior to the fall. Her knee was swollen and painful at the time of her initial physical examination. Radiographs (Fig 1) of the knee were performed, revealing a mixed lytic and sclerotic lesion measuring 3.5 cm craniocaudal (CC) x 2 cm antero-posterior (AP) x 3.5 cm transverse (TV) involving the epiphysis and metaphysis of the right lateral femoral condyle. Further characterization was performed with MRI (Fig 2), which was interpreted as a distal femur mass lesion complicated by lateral condyle displaced pathological fracture.

Percutaneous bone biopsy performed two weeks after initial presentation yielded viable trabecular bone. Results were negative for infection or neoplasm, and the specimen was felt to be non-diagnostic as the histologic changes were discordant with radiographic findings.

Evaluation with bone scan (Fig 3) was performed one month after discovery of the initial lesion in order to identify additional pathologic foci. The bone scan demonstrated

increased activity in the lateral aspect of the distal epiphysis and metaphysis of the right femur.

Due to the discordant results from the initial percutaneous bone biopsy, as well as the continued concern about malignancy, an open bone biopsy was performed approximately six weeks after discovery of the lesion, which demonstrated benign fibrovascular proliferation with cartilaginous and osseous metaplasia, without evidence of malignancy.

At six month follow up, a repeat MRI with and without contrast of the right knee (Fig 4) was performed, and demonstrated progressive remodeling of displaced fracture through the posterior aspect of the lateral femoral condyle.

A follow-up right knee MRI (Fig 7) at nine months revealed expected post-operative changes at the biopsy site of the lateral femoral condyle, as well as progressive remodeling of the fracture and ossification of the epiphysis with resolution of the mass-like lesion. Additionally, during this follow-up visit, the patient began to report mild right ankle pain. Radiographs of the right ankle (Fig 5) demonstrated swelling of the ankle without fracture or dislocation. Ankle MRI (Fig 6) was performed, showing advanced osteoarthritis of the

posterior subtalar joint as well as extensive bone marrow edema of the talus and cystic change in the posterior facet of the talus. Exuberant bone marrow edema was present in the lateral and medial malleoli, calcaneus and cuboid, as well as the tibiotalar and subtalar joints.

Once the ankle joint became involved, there was suspicion of a systemic inflammatory disease. Given the multiple bone biopsies without malignant pathology and multiple joint involvement, oligo-articular juvenile idiopathic arthritis was the presumptive diagnosis. The auto-antibodies and labs typically associated with juvenile arthritis were negative, including anti-nuclear antibodies (ANA), rheumatoid factor, anti-cyclic citrullinated peptide (anti-CCP) antibody and human leukocyte antigen (HLA) B27. The patient was treated with methotrexate and prednisone without any clinical improvement. She underwent intra-articular corticosteroid injections of the right ankle and knee, which resulted in mild improvement of joint pain and swelling. Given the patient's clinical history, absence of the expected severe pain with the advanced osteoarthritis and fractures, as well as the lack of response to methotrexate and steroids, the diagnosis was in question. Further history was later obtained that during her childhood, she used to pull out her eyelashes and not cry as much as other children in response to pain. Hence, a diagnosis of congenital indifference to pain was pursued. Subsequently, genetic analysis was performed, revealing a mutation in the SCN9A gene, confirming the diagnosis of congenital insensitivity to pain.

## DISCUSSION

### Etiology and Demographics

Congenital insensitivity to pain (CIP), also known as congenital indifference to pain, was first described in the literature by Dearborn in 1932 [1]. Since then, less than 50 cases of congenital indifference to pain have been published in the medical literature. A total of approximately 150 total cases have been reported when combined with the more studied variant, congenital insensitivity to pain with anhidrosis (CIPA) [2].

Congenital indifference to pain has been shown to follow an autosomal recessive pattern

of inheritance [3]. It belongs to a larger family of Hereditary Sensory and Autonomic Neuropathies (HSAN) [4]. Congenital indifference to pain is caused by a mutation in the SCN9A gene, which codes for the sodium channel Nav 1.7 protein. A multitude of mutations can occur at the SCN9A gene, and this may result in vastly different outcomes affecting sodium channel NaV1.7.

The precise function of the NaV1.7 protein is unclear. However, it is known to be involved in generation of action potentials for a variety of sensory and autonomic functions. This explains why different mutations in the SCN9A gene can result in a wide variety of clinical presentations, ranging from insensitivity to pain to hyperalgesia or anosmia [5]. The most severe variant of SCN9A mutation is congenital insensitivity to pain with anhidrosis, a fatal variant which causes brain

damage, mental retardation, unexplained fevers, and eventually death by hyperpyrexia [6].

### Clinical and Imaging Findings

Our patient had normal cognitive and motor development, sweat and lacrimal

glands function, and sympathetic skin responses. The patient did not have any unexplained bouts of fever. While many patients may go undetected with multiple injuries for many years, our case was unique in the sense that the patient presented with a single sub-acute fracture due to the fact that she had at least some preserved sensation of pain.

In some cases, congenital indifference to pain may be suspected as early as infancy when painful stimuli like the pin prick from blood draw evoke no response [7]. One study describes a patient with incomplete congenital indifference to pain who was first suspected of the disorder when she sustained a painless corneal abrasion at the age of 6 months. At the age of two years, she suffered second degree burns to her hand and did not exhibit pain response. She first showed signs of pain when she acquired otitis media later in life. Sural nerve biopsy in that particular patient was normal, an expected finding with pain insensitivity syndromes as the nerves are histologically intact [3].

As with most cases of congenital indifference to pain, a detailed and accurate history is essential to avoid unnecessary workup as well as to clinch the diagnosis. Historically, peripheral nerve biopsy was performed to exclude other mimickers of the disease [7]. Electroencephalogram, cerebrospinal fluid analysis, and sensory and motor nerve conduction studies were found to be normal in a majority of patients [8]. Now that genetic testing has become available in many clinical settings, gene analysis has become the gold standard for establishing the diagnosis [5].

### Treatment and Prognosis

Prevention and early detection of injury is of upmost importance in these patients in order to avoid morbidity related to undetected injuries. Once the diagnosis has been established, it is important to have a high clinical suspicion for fractures, even in the setting of minimal or complete lack of pain. Although no formal guidelines for treatment have been established, liberal imaging at sites of potential injury is recommended as the pain response is variable and unreliable. According to American College of Radiology (ACR) Appropriateness Criteria, plain radiographs are the study of choice if fracture is suspected, and can be applied in this setting as well [9]. Prevention plays a key role in management of these patients. Custom fitted shoes and protective padding to prevent ulcers should be provided. Regular follow up is recommended, as well as prompt medical and surgical attention if necessary [10].

### Differential Diagnosis

Differential considerations vary based on if the presentation is monoarticular or polyarticular. Our patient initially presented with an isolated lesion with pathologic fracture, which led to workup for a neoplasm. Malignancy was eventually ruled out based on histologic sampling.

Inflammatory arthropathy is also a consideration, as in our case, when inflammatory changes predominate on imaging or there is polyarticular involvement. An additional consideration is neuropathic joint related to chronic neuropathy caused by a long standing illness such as diabetes or vascular disease. While the patient did have findings in the ankle consistent with neuropathic joint, she lacked additional findings of diabetes or vascular disease. Fractures secondary to non-accidental injury should always be considered in young children, though it can be differentiated from congenital indifference to pain if the patient has a normal sensory examination. Given the age of late presentation of our patient, and lack of associated cutaneous stigmata, spina bifida aperta was not a consideration, though it should be strongly considered in a patient presenting in infancy. Eventually, after excluding all other possibilities, the correct diagnosis of congenital insensitivity to pain was confirmed by SCN9A gene testing.

#### Clinical Application of SCN9A Mutation

Clinical applications are already being developed to lower analgesic doses in post-operative patients with SCN9A gene mutations. In a study that enrolled 200 patients who underwent pancreatectomy, those found to have the 3312T single nucleotide polymorphism (present in approximately 10% of the population) were found to require 30% less opioids and were at six-fold less risk of inadequate analgesia than those with the 3312G allele [11]. Further research has the potential to profoundly impact peri-operative and post-operative pain management. Additionally, it is critical to differentiate between different subtypes of the disease, as individuals suffering from the CIPA variant will have impaired thermoregulation and are at increased risk for malignant hyperthermia. Given the overall rarity of the disease, genetic testing of the entire population prior to operation is not feasible, though a thorough history may prompt testing on an individual basis, and can be useful for both peri- and post-operative pain management [12].

#### TEACHING POINT

Congenital indifference to pain is a rare and debilitating disorder that impairs the ability to detect pain. Many patients will present in their early years of life with healing fractures, which are often radiographically indistinguishable from aggressive neoplasms. Once appropriate workup has been completed to exclude a neoplasm, genetic testing of SCN9A gene may reveal the diagnosis of congenital indifference to pain, and help implement early preventative measures to avoid further morbidity.

#### REFERENCES

1. Dearborn GVN. A case of congenital pure analgesia. *Journal Nerv Ment Dis* 1932; 75: 612-15.
2. Schwarzkopf R, Pinsk V, Weisel Y, Atar D, Gorzak Y. Clinical and genetic aspects of congenital insensitivity to pain with anhydrosis. *Harefuah* 2005 June; 144(6): 433-7, 453, 452. PMID 15999564
3. Staud R, Price DD, Janicke D Andrade E, et al. Two Novel Mutations of SCN9A (NaV1.7) are Associated with Partial Congenital Insensitivity to Pain. *Eur J Pain* 2011 March; 15(3): 223-230. PMID 20692858
4. Kumar BP, Sudhaker S, Prabhat MPV. Case report: Congenital Insensitivity to Pain. *Online Journal of Health and Allied Sciences* 2010; Volume 9, Issue 4.
5. Shorer Z, Wajsbrot E, Liran TH, Levy J, Parvari R. A Novel Mutation in SCN9A in a Child with Congenital Insensitivity to Pain. *Pediatric Neurology* 2014; 50: 73-76. PMID 24188911
6. Yang L, Ji SF, Yue RJ, Cheng JL, Niu JJ. Old fractures in two patients with congenital insensitivity to pain with anhydrosis: radiologic findings. *Clinical Imaging* 2013; 37: 788-90. PMID 23478071
7. Swanson AG, Buchan GC, Alvord EC. Anatomic Changes in Congenital Insensitivity to Pain. *JAMA Neurology* 1965; Volume 12. PMID 14224855
8. Edwards-Lee TA, Cornford ME, Yu KTT. Congenital Insensitivity to pain and anhydrosis with mitochondrial and axonal abnormalities. *Pediatric Neurology* 1997; 17: 356-61. PMID 9436803
9. ACR Appropriateness Criteria for Musculoskeletal Imaging. American College of Radiology. Accessed on February 21, 2014. <http://www.acr.org/Quality-Safety/Appropriateness-Criteria/Diagnostic/Musculoskeletal-Imaging>
10. Karthikeyan M, Sreenivas T, Menon J, Patro KD. Congenital insensitivity to pain and anhydrosis: a report of two cases. *Journal of Orthopaedic Surgery* 2013; 21(1): 125-128. PMID 23630006
11. Duan G, Xiang G, Zhang X, Yuan R, Zhan H, Qi D. A Single-nucleotide Polymorphism in SCN9A May Decrease Postoperative Pain Sensitivity in the General Population. *Anesthesiology* 2013; 118: 436-4. PMID 23364568
12. Parrott LM. Anesthetic management of a patient with congenital insensitivity to pain: a case report. *AANA Journal* 2013 October; 81(5): 376-8. PMID 24354073

FIGURES



**Figure 1:** 8 year old female with congenital indifference to pain. FINDINGS: Initial frontal and lateral radiographs of the right knee reveal mixed lytic and sclerotic lesion measuring 3.5 x 2 x 3.5 cm involving the epiphysis and metaphysis of the lateral femoral condyle with fragmentation and irregularity of the lateral femoral condyle articular surface (black arrows). TECHNIQUE: Fig 1a. Frontal: kVp 70, mA 478, mAs 3. Fig 1b. Lateral: kVp 70, mA 497, mAs 3

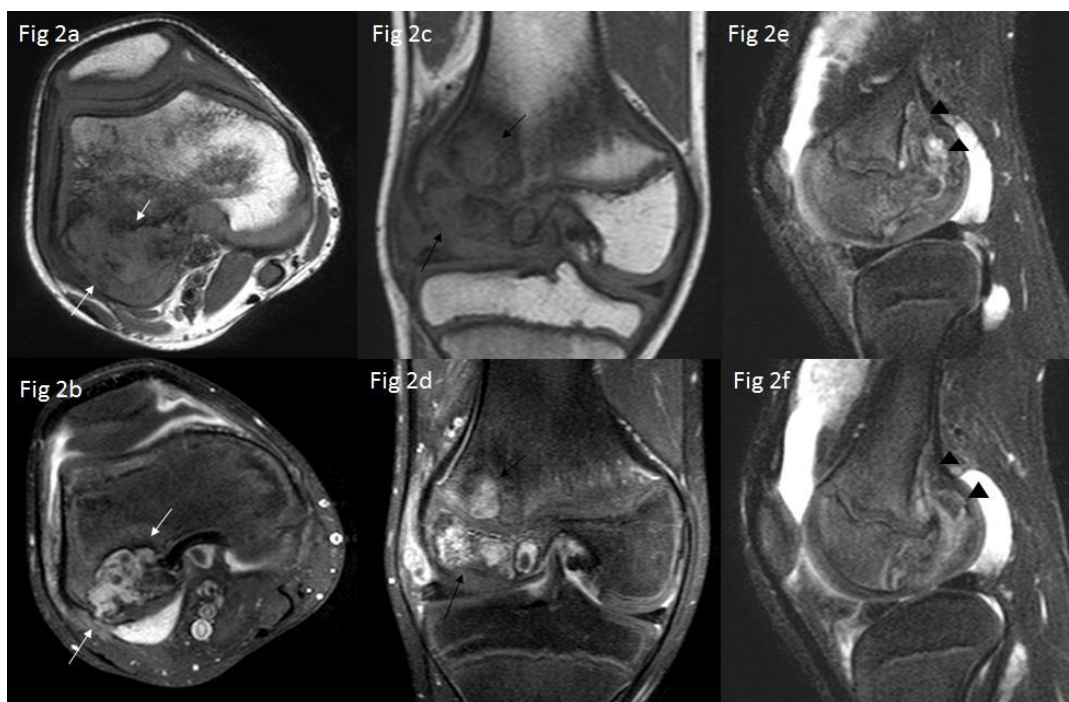


**Figure 2:** 8 year old female with congenital indifference to pain. FINDINGS: Initial MRI with and without contrast of the right knee. Axial T1 precontrast (Fig 2a) and post-contrast (Fig 2b) demonstrate a heterogeneous lesion measuring 3.5 x 2 x 3.5 cm in the posterior aspect of the lateral femoral condyle that is heterogeneously iso- and hypointense relative to skeletal muscle on T1 imaging with heterogeneous, septal enhancement (white arrows). Coronal T1 precontrast (Fig 2c) and post-contrast (Fig 2d) demonstrate the lesion spanning from the epiphysis through the physis into the metaphysis (black arrows). Focal areas of non-enhancement of the lesion are present along the articular surface. Sagittal T2 non-contrast sequences (Fig 2e-f) demonstrate the lesion as being hyper-intense to muscle with a few small cystic areas. Subperiosteal extension of soft tissue causes scalloping of the posterior aspect of the distal femur metaphysis (black arrowheads). The final impression was lateral femoral condyle displaced pathological fracture secondary to an underlying mass lesion. TECHNIQUE: Scanner: Philips Achieva. Magnet: 1.5 Tesla Scanner. Coil used: SENSE-Knee-8. Fig 2a. Axial T1 non-contrast: TR 603, TE 20, slice thickness 2.5 mm, slice spacing 2.75 mm. Fig 2b. Axial T1 post contrast: TR 621, TE 20, slice thickness 2.5 mm, slice spacing 3.1 mm. Fig 2c. Coronal T1 pre contrast: TR 498, TE 20, slice thickness 2.5 mm, slice spacing 3.1 mm. Fig 2d. Coronal T1 post contrast: TR 499, TE 20, slice thickness 2.6 mm, slice spacing 3.2 mm. Fig 2e-f. Sagittal T2: TR 3011, TE 65, slice thickness 2.6 mm, slice spacing 3.2 mm.

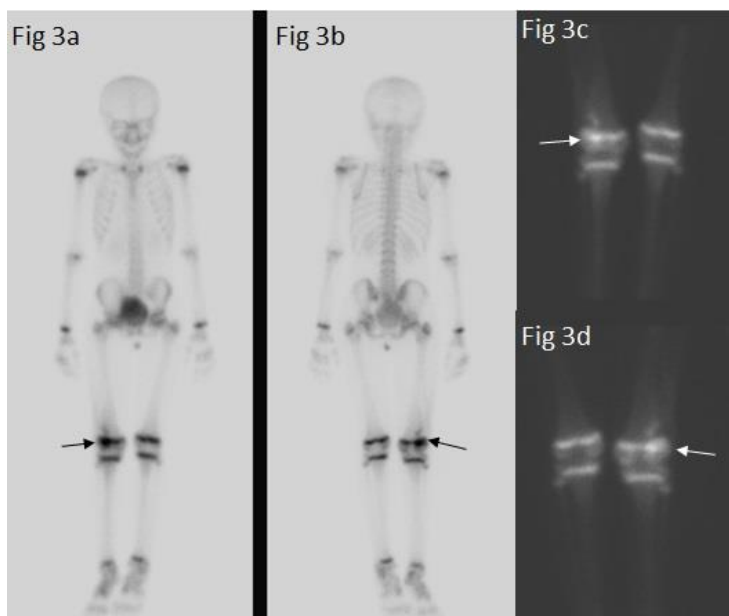


**Figure 3 (left):** 8 year old female with congenital indifference to pain.

**FINDINGS:** Bone scan was performed one month after presentation. Anterior (Fig 3a) and posterior (Fig 3b) images taken 4 hours after administration of technetium 99m MDP demonstrate increased activity in the lateral aspect of the distal epiphysis and metaphysis of the right femur (black arrows). No other areas of pathologically increased activity are identified. Dedicated anterior (Fig 3c) and posterior (Fig 3d) views of the knees show the same finding (white arrows).

**TECHNIQUE:** 4 hour delayed whole body and focused planar images after administration of 15 mCi of technetium 99m MDP



**Figure 4:** 8 year old female with congenital indifference to pain. **FINDINGS:** At six month follow up, a repeat MRI with and without contrast of the right knee was performed. Axial T1 post-contrast with fat saturation (Fig 4a) and axial proton density fat saturated images (Fig 4b) demonstrate progressive remodeling of the displaced fracture through the posterior aspect of the lateral femoral condyle (thin black arrows). There is progressive ossification of the epiphysis with areas in the lateral femoral condyle lesion now demonstrating architecture that resembles normal trabecular bone. Coronal T1 non-contrast image (Fig 4c) demonstrates interval progression of ossification of the lateral femoral condyle with interval development of small areas of fat signal intensity and trabecular architecture in the region of the lateral femoral condyle lesion. Coronal proton density fat saturated image (Fig 4d) reveals that the previously described areas of cystic change have resolved, with overall decrease of the T2 hyperintense signal indicating decreased edema. Expected post-operative changes at the biopsy site (thick black arrow on Fig 4c-d). **TECHNIQUE:** Scanner: Philips Achieva. Magnet: 1.5 Tesla Scanner. Coil used: SENSE-Knee-8. Contrast: 4 mL Omniscan. Fig 4a. Axial T1 fat suppressed turbo spin echo post contrast: TR 695, TE 20, slice thickness 4mm, slice spacing 5 mm. Fig 4b. Axial PD fat suppressed: TR 3699, TE 4, slice thickness 4 mm, slice spacing 5mm. Fig 4c. Coronal T1 non contrast: TR 821, TE 15, slice thickness 2.5 mm, slice spacing 2.75 mm. Fig 4d. Coronal PD fat suppressed non-contrast: TR 4837, TE 30, slice thickness 2.5, slice spacing 2.75.



**Figure 5:** 8 year old female with congenital indifference to pain. FINDINGS: At her nine month followed up the patient began to complain of right ankle pain. AP (Fig 5a) and lateral (Fig 5b) radiographs of the ankle demonstrate swelling of the soft tissues lateral to the ankle joint (white arrow) and tibiotalar joint effusion (black arrow) with normal appearing osseous structures. TECHNIQUE: Fig 7a. Frontal: kVp 64, mAs 4. Fig 7b. Lateral: kVp 64, mAs 4.

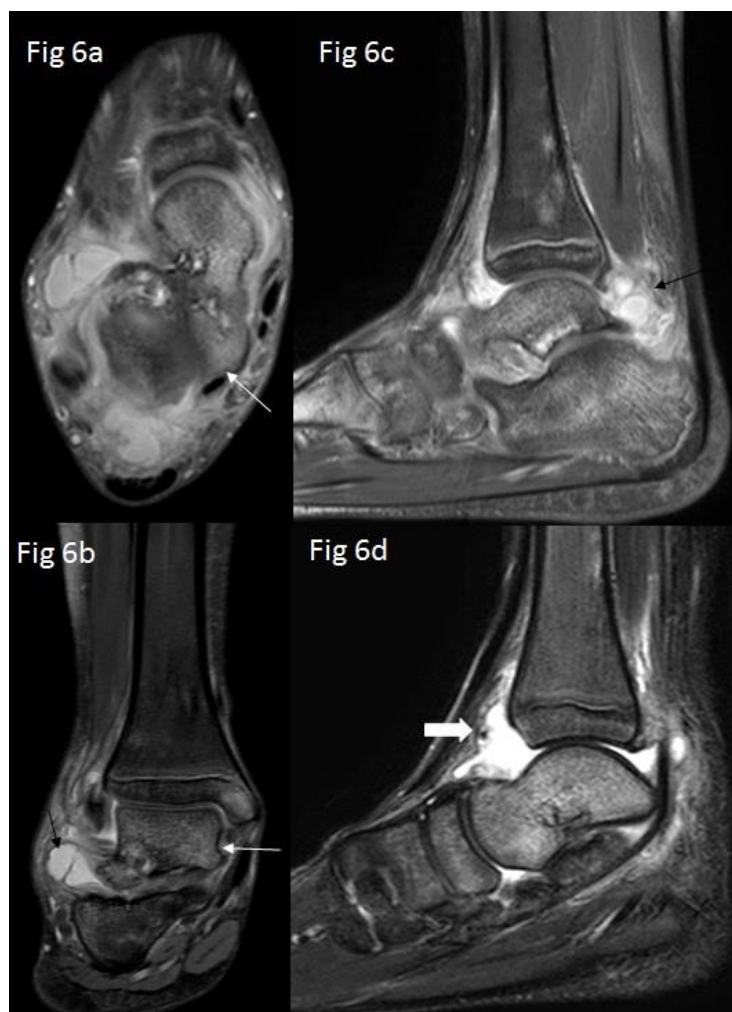


**Figure 6 (left):** 8 year old female with congenital indifference to pain. FINDINGS: Initial ankle MRI in axial fat saturated proton density (PD) (Fig 6a) and coronal fat saturated proton density (Fig 6b) echo sequences demonstrates extensive marrow edema of the talus (thin white arrows on image 6a and 6b) and cystic change in the posterior facet of the talus. There is additional exuberant bone marrow edema at the lateral malleolus, medial malleolus (white arrowhead on image 6b), calcaneus, and cuboid. Coronal fat saturated PD (Fig 6b) and sagittal T1 fat suppressed turbo spin echo post contrast (Fig 6c) show exuberant synovitis of the tibiotalar and subtalar joints (black arrows on image 6b and 6c). A large ankle effusion (thick white arrow on image 6d) is seen on sagittal STIR images (Fig 6d). TECHNIQUE: Scanner: Philips Achieva. Magnet: 1.5 Tesla Scanner. Coil used: Magnet: 1.5 Tesla Scanner. SENSE-FT Ankle8. Contrast used: 5mL Omniscan. Fig a. Axial PD fat suppressed: TR 4406, TE 30, slice thickness 3 mm, slice spacing 3.1 mm. Fig 6b. Coronal PD fat suppressed: TR 4506, TE 30, slice thickness 3 mm, slice spacing 3.3 mm. Fig 6c. Sagittal T1 fat suppressed turbo spin echo post contrast: TR 633, TE 20, slice thickness 2.5 mm, slice spacing 2.75 mm. Fig 6d. Sagittal STIR: TR 3941, TE 60, slice thickness 2.5 mm, slice spacing 2.75 mm.

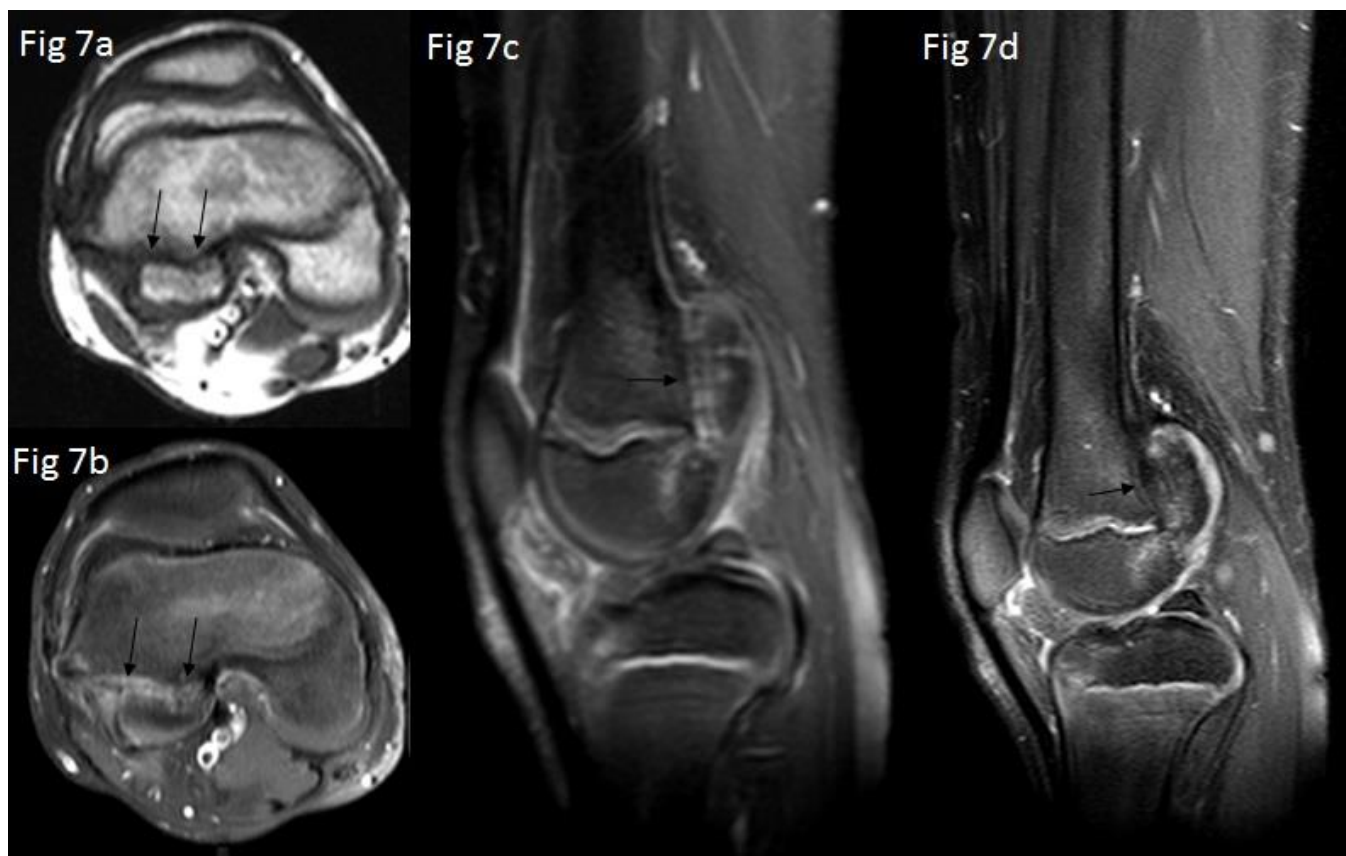


**Figure 7:** 8 year old female with congenital indifference to pain. FINDINGS: MRI with and without contrast of the right femur at nine month follow up. Non-contrast axial T1 turbo spin echo (Fig 7a) and post-contrast axial T1 turbo spin echo fat saturated (Fig 7b) images demonstrate progressive healing of the displaced fracture through the lateral femoral condyle as well as progressive ossification of the lateral femoral condyle epiphysis (black arrows). There is normal marrow signal and trabecular architecture through almost the entire lateral femoral condyle with a small amount of residual abnormal signal adjacent to the fracture site. These changes are also annotated on post-contrast sagittal T1 fat saturated (Fig 7c) and T2 TSE fat saturated (Fig 7d) images. On T1 contrast enhanced fat suppressed sequences (Fig 7e), no fracture or pathologic enhancement is noted. TECHNIQUE: Scanner: Philips Achieva. Magnet: 1.5 Tesla Scanner. Coil used: SENSE-Cardiac. Contrast used: 5mL Omniscan. Fig 7a. Axial T1 TSE: TR 237, TE 20, slice thickness 6 mm, slice spacing 7mm. Fig 7b. Axial T1 TSE fat suppressed post contrast: TR 618, TE 20, slice thickness 6mm, slice spacing 7mm. Fig 7c. Sagittal T1 fat suppressed post contrast: TR 516, TE 20, slice thickness 5.5 mm, slice spacing 6 mm. Fig 7d. Sagittal T2 TSE fat suppressed: TR 3500, TE 60, slice thickness 5mm, slice spacing 6mm. Fig 7e. Coronal T1 TSE fat suppressed post contrast: TR 620, TE 20, slice thickness 6 mm, slice spacing 7 mm.

www.RadiologyCases.com

<b>Etiology</b>	Congenital autosomal recessive disorder
<b>Incidence</b>	Very rare. With less than 150 reported cases, the incidence is less than 1/1,000,000
<b>Gender Ratio</b>	Equally distributed among male and female
<b>Age Predilection</b>	None
<b>Risk Factors</b>	None. The disease is congenital.
<b>Treatment</b>	Preventative care such as custom fit shoes and protective padding. Close clinical follow-up is necessary for early detection and treatment of injury
<b>Prognosis</b>	Patients that have access to medical care can have a near normal lifespan.
<b>Findings on Imaging</b>	The patient may present with old healed fractures and/or new fractures in different stages of healing depending on when they present.
<b>Findings on Pathology</b>	Bone biopsy will show healing bone.

**Table 1:** Summary table for congenital indifference to pain

Differential diagnosis	X-ray	MRI	Bone scan
<b>Congenital Insensitivity to Pain, Congenital Insensitivity to Pain with anhydrosis</b>	Acute, sub-acute, and healed fractures.	Better characterization of fractures. MRI can also be misleading if obtained for fracture	Increased uptake in all 3 phases
<b>Osteosarcoma</b>	Bony sclerosis, periosteal thickening and adjacent soft tissue mass.	Aggressive, heterogeneous mass	Increased uptake in all 3 phases
<b>Juvenile Idiopathic Arthritis</b>	Bony erosion, effusions, and progressive joint destruction	Joint effusions, tenosynovitis, marrow edema, erosions	Increased blood flow and radiotracer accumulation in and around joints
<b>Non-accidental injury</b>	Acute, sub-acute, and healed fractures.	Better characterization of fractures. MRI can also be misleading if obtained for fracture.	Increased uptake in all 3 phases
<b>Spina Bifida Aperta</b>	Incomplete posterior element fusion in lumbosacral spine with wide eversion of lamina	Wide spinal dysraphism, flared laminae, and low-lying cord	N/A
<b>Neuropathic (Charcot) Joint</b>	Large joint effusion, cartilage destruction, joint disorganization	Osseous destruction of both sides of joint, debris within large joint effusion	Increased uptake in all 3 phases

**Table 2:** Differential diagnosis table for congenital indifference to pain

ABBREVIATIONS

ACR = American College of Radiology  
 ANA = Anti-nuclear antibody  
 Anti-CCP = Anti-cyclic citrullinated peptide  
 AP = Anterior-posterior  
 CC = Craniocaudal  
 CIP = Congenital indifference to pain  
 CIPA = Congenital indifference to pain with anhydrosis  
 FS = Fat saturated  
 HLA = Human Leukocyte Antigen  
 HSAN = Hereditary Sensory and Autonomic Neuropathies  
 kVp = Peak kilovoltage  
 mAs = Milliampere seconds  
 mCi = Millicurie  
 MRI = Magnetic resonance imaging  
 PD = Proton density  
 SCN9A = Sodium channel, voltage-gated, type IX, a subunit  
 STIR = Short TI inversion recovery  
 TE = Echo time  
 Technetium 99m MDP = Technetium 99 metastable methylene di-phosphnate  
 TR = Relaxation time  
 TSE = Turbo spin echo  
 TV = Transverse

KEYWORDS

Congenital indifference to pain; congenital insensitivity to pain; congenital insensitivity to pain with anhydrosis; congenital pure analgesia; MRI; bone scan; neuropathic arthropathy; inflammatory arthropathy

**Online access**

This publication is online available at:  
[www.radiologycases.com/index.php/radiologycases/article/view/2194](http://www.radiologycases.com/index.php/radiologycases/article/view/2194)

**Peer discussion**

Discuss this manuscript in our protected discussion forum at:  
[www.radiopolis.com/forums/JRCR](http://www.radiopolis.com/forums/JRCR)

**Interactivity**

This publication is available as an interactive article with scroll, window/level, magnify and more features.  
 Available online at [www.RadiologyCases.com](http://www.RadiologyCases.com)

Published by EduRad



[www.EduRad.org](http://www.EduRad.org)